

Glycated Fibroblast Growth Factor-2 Is Quickly Produced *in Vitro* upon Low-Millimolar Glucose Treatment and Detected *in Vivo* in Diabetic Mice

Francesco Facchiano, Daniela D'Arcangelo, Katia Russo, Vincenzo Fogliano, Carmela Mennella, Raffaele Ragone, Giovanna Zambruno, Virginia Carbone, Domenico Ribatti, Cesare Peschle, Maurizio C. Capogrossi, and Antonio Facchiano

Dipartimento di Ematologia Oncologia e Medicina Molecolare (F.F., C.P.), Istituto Superiore di Sanità, I-00161 Roma, Italy; Laboratorio di Patologia Vascolare (F.F., D.D., K.R., M.C.C., A.F.), and Laboratorio di Biologia Molecolare e Cellulare (G.Z.), Istituto Dermopatico dell'Immacolata-IDI, Istituto di Ricovero e Cura a Carattere Scientifico, I-00167 Roma, Italy; Dipartimento di Scienza degli Alimenti (V.F., C.M.), Università di Napoli "Federico II", I-80055 Portici, Italy; Dipartimento di Biochimica e Biofisica (R.R.), Seconda Università di Napoli, I-80138 Napoli, Italy; Istituto di Scienze dell'Alimentazione (V.C.), Consiglio Nazionale delle Ricerche, I-83100 Avellino, Italy; and Dipartimento di Anatomia Umana e Istologia (D.R.), Policlinico, I-70124 Bari, Italy

Angiogenesis impairment in hyperglycemic patients represents a leading cause of severe vascular complications of both type-1 and -2 diabetes mellitus (DM). Angiogenesis dysfunction in DM is related to glycemic control; however, molecular mechanisms involved are still unclear. Fibroblast growth factor-2 (FGF-2) is a potent angiogenic factor and, according to previous evidence, may represent a key target of molecular modifications triggered by high-sugar exposure. Therefore, the purpose of this study was to investigate whether short incubation with hyperglycemic levels of glucose affected FGF-2 and whether glucose-modified FGF-2 was detectable *in vivo*. Biochemical analyses carried out with SDS-PAGE, fluorescence emission, mass-spectrometry, immunoblot, and competitive ELISA experiments demonstrated that human FGF-2 undergoes a rapid and specific glycation upon 12.5–50 mM glucose exposure. In addition, FGF-2 exposed for 30 min to 12.5 mM glucose lost mitogenic and chemotactic activity in a time- and dose-dependent manner. Under similar

conditions, binding affinity to FGF receptor 1 was dramatically reduced by 20-fold, as well as FGF receptor 1 and ERK-1/2 phosphorylation, and FGF-2 lost about 45% of angiogenic activity in two different *in vivo* angiogenic (Matrigel and chorioallantoic-membrane) assays. Such glucose-induced modification was specific, because other angiogenic growth factors, namely platelet-derived growth factor BB and placental-derived growth factor were not significantly or markedly less modified. Finally, for the first time, glycated-FGF-2 was detected *in vivo*, in tissues from hyperglycemic nonobese diabetic mice, in significantly higher amounts than in normoglycemic mice. In conclusion, hyperglycemic levels of glucose may strongly affect FGF-2 structure and impair its angiogenic features, and endogenous glycated-FGF-2 is present in diabetic mice, indicating a novel pathogenetic mechanism underlying angiogenesis defects in DM. (*Molecular Endocrinology* 20: 2806–2818, 2006)

MOLECULAR MECHANISMS underlying vascular complications in diabetes mellitus (DM) are still not completely elucidated and represent an emerging field of investigation, with potentially large clinical and social impact. Previous studies indicated close relationships between glycemic control and incidence/severity of DM complications (1–6) and serum levels of glycation products were related to the development of

vascular complications in type 1 and 2 DM (7–9). Protein glycation depends on glucose concentration and on levels of triose phosphate metabolites (10), deoxyglucosones (11), and other compounds and sugars. These compounds act *per se* or generate other potent glyating agents such as methylglyoxal (12) or glyoxal, which is formed under physiological conditions via oxidative degradation of Amadori products (13) or lipid

First Published Online July 13, 2006

Abbreviations: AGE, Advanced glycation end; BAEC, bovine aortic endothelial cell; CAM, chorioallantoic membrane; DM, diabetes mellitus; EC, endothelial cell; FCS, fetal calf serum; FGF-2, fibroblast growth factor-2; FGFR1, FGF receptor 1; HUVEC, human umbilical vein endothelial cell; MALDI/MS, matrix-assisted laser desorption ionization mass spectrometry; NOD, nonobese diabetic; PIGF, placental growth factor;

PDGF-BB, platelet-derived growth factor-BB; RNase, ribonuclease; RU, resonance unit; SPR, surface plasmonic resonance; TUNEL, terminal deoxynucleotide transferase-mediated deoxyuridine triphosphate nick-end labeling.

Molecular Endocrinology is published monthly by The Endocrine Society (<http://www.endo-society.org>), the foremost professional society serving the endocrine community.

peroxidation (14). Therefore, the serum molecules able to modify proteins via a glycation process are more than just glucose, and glycemic level only, in part, describes, in DM patients, the concentration of effective serum glycyating molecules.

Hyperglycemia promotes endothelial cells (ECs) dysfunction in insulin-dependent and insulin-independent DM and is a major causal factor in development of macro- and microvascular diseases (1–4). Endothelial dysfunction in DM leads to a severe angiogenesis impairment, according to clinical as well as experimental studies (15–18); further, angiogenesis impairment in hyperglycemic DM patients may lead to serious skin ulcers and amputation, or increased morbidity and mortality due to coronary artery disease. Molecular mechanisms underlying these angiogenic defects are still not completely clarified. However, it is known that elevated glucose serum levels may induce protein nonenzymatic glycosylation (glycation) where free amino groups belonging to lysine or arginine residues interact with reducing sugars forming unstable Schiff bases which, in turn, through the Amadori rearrangement, proceed toward formation of advanced glycation end (AGE) products (19, 20). Several proteins, including extracellular matrix proteins, serum albumin, hemoglobin, ribonuclease (RNase), crystallins, lysozyme, and β -lactoglobulin, undergo such nonenzymatic modification, and precipitate as insoluble material with capillary basement membrane thickening, a hallmark of diabetic microangiopathy (7, 21–24). Glycation products accumulation may be induced by glucose, as well as by many other reducing molecules elevated in DM, and has been involved in the etiology of both micro- and macrovascular complications and EC dysfunction of DM (7, 25–32). Further, accumulation of glycated proteins such as hemoglobin is considered a marker of the hyperglycemic history and a proof of the glycation occurring *in vivo*. Interestingly, other proteins have been reported to be glycated *in vitro* (21, 33, 34), including growth factors and enzymes (7), upon long-term exposure to high-sugar concentrations (*i.e.* 24- to 48-h incubation with 200 mM or higher concentrations of sugars like glucose-6-phosphate, glyceraldehyde-3-phosphate). The effects of very short incubations with low-glucose concentrations, comparable to those found in hyperglycemic conditions, on regulatory proteins such as angiogenic growth factors, and the direct determination *in vivo* of their glycation were never reported. In the present study, we report for the first time the detection of glycated fibroblast growth factor-2 (FGF-2) *in vitro* upon experimental conditions, namely 30–60 min incubation with 12.5–50 mM glucose, comparable to those present in hyperglycemia and in DM patients, showing a significant functional impairment as compared with unglycated FGF-2. Furthermore, for the first time direct evidence of *in vivo* FGF-2 glycation is reported in the present study. Therefore, these data strongly support the existence of a novel pathogenetic mechanism underlying angiogenesis impairment and

vascular complications in DM, specifically involving both proliferative/chemotactic and angiogenic activities of FGF-2.

RESULTS

Biochemical Modifications Induced by Glucose Incubation

Hyperglycemia in DM patients usually ranges from 6–30 mM, and in some cases it may reach 55 mM in hyperosmolar hyperglycemic nonketotic diabetic patients (35). Therefore, to mimic a pathological context corresponding to DM, in this study FGF-2 was incubated with glucose concentrations ranging from 12.5 to 50 mM, in most experiments. We first carried out biochemical studies, namely SDS-PAGE analysis under denaturing conditions and mass spectrometry analysis, to evaluate the structural modifications of FGF-2 incubated with glucose. FGF-2 was incubated with 50 mM glucose added with tracing amounts of [14 C]glucose, and denaturing SDS-PAGE analysis was carried out, followed by autoradiography. A direct binding of the [14 C]glucose to monomer FGF-2 was detected at 1 h incubation; upon longer incubation time, it paralleled the formation of labeled high molecular mass (HMM) complexes (Fig. 1A). In the range of 40–90 kDa, glucose incubation induced the formation of a faint labeled smeared band (data not shown). Upon longer time exposure (48–96 h or longer), or higher sugar concentration, both the HMM complexes and the smeared band were more evident (data not shown). The smeared band and the aggregates at high molecular mass, observed under denaturing electrophoretic conditions, are very similar to those described for other proteins, *e.g.* ovalbumin, when exposed to the nonenzymatic glycation reaction (36).

In mass spectrometry studies, FGF-2 incubated with 50 mM glucose showed a marked mass shift (Fig. 1B) corresponding to an approximately 160-Da increase of mass, indicating the formation of glucose-containing adducts, likely due to glycation. Mannitol was used as inactive, isoosmotic control and gave no mass shift. In additional mass spectrometry studies, glycated FGF-2 was cleaved by cyanogen bromide treatment according to a published protocol (37) to localize where the sugar-induced chemical modification occurs. Preliminary results indicate that one residue in the C-terminal fragment of FGF-2 (between residues 85 and 150) is the most rapidly modified by glucose with an approximately 160-Da mass shift, suggesting the formation of a glycated adduct (data not shown). As an additional approach, the intrinsic fluorescence of FGF-2 was then investigated upon 30 and 60 min incubation with glucose, using mannitol as a control. Figure 2A shows that, upon excitation at 278 nm, the maximum of the fluorescence spectrum in the absence of glucose was centered at about 340 nm,

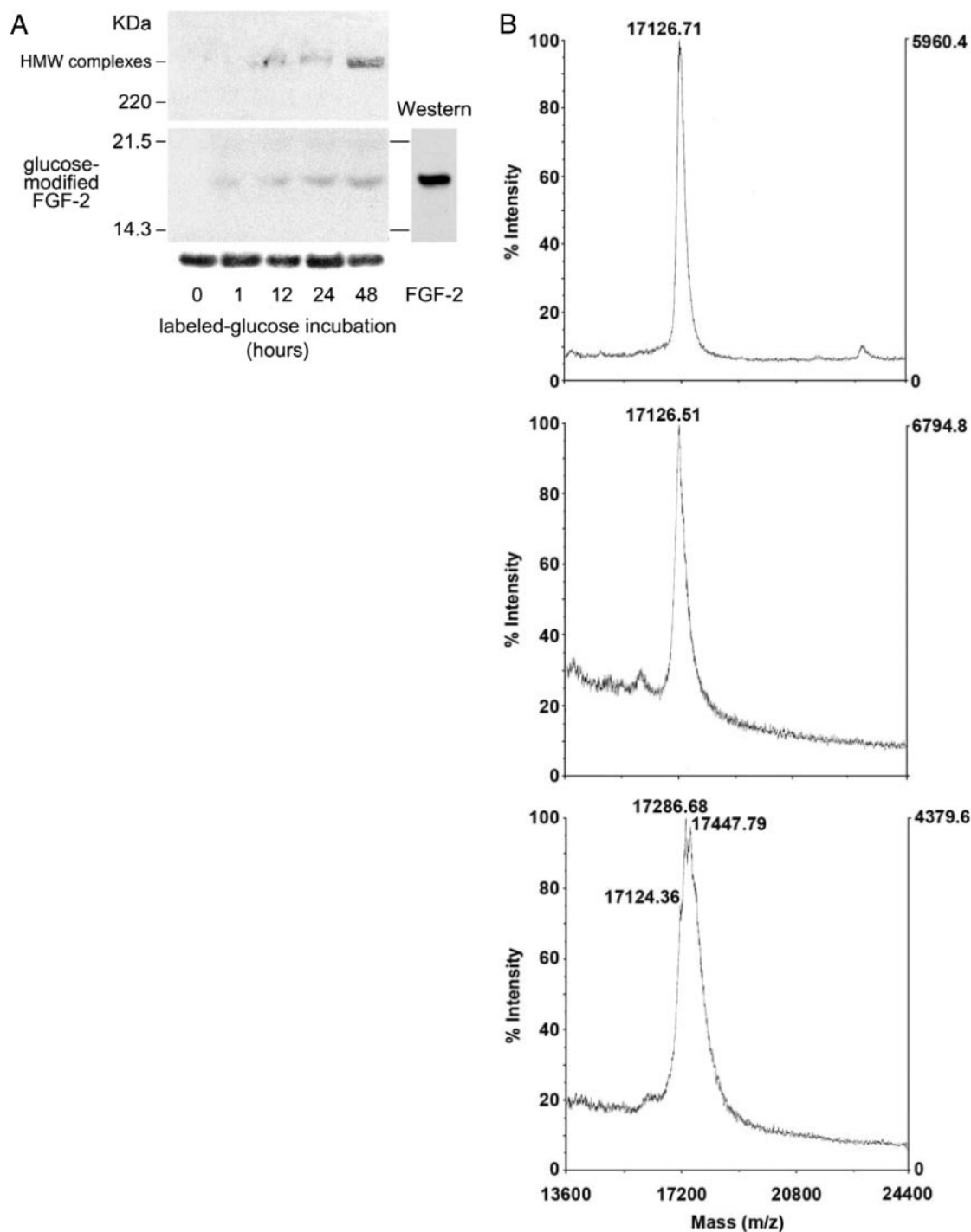


Fig. 1. Biochemical Analysis of Glucose-Incubated FGF-2

A, Autoradiographic SDS-PAGE analysis. FGF-2 (1 μ g) incubated with 50 mM glucose added with trace amounts of [14 C]glucose was subjected to SDS-PAGE followed by autoradiography (*upper and middle panels*). High molecular mass (HMW) complexes at the beginning of the resolving gel are marked. An equal amount of FGF-2 loaded in the gel was assayed by Western blot (*lower and righthand panels*). B, Mass spectrometry analysis: FGF-2 (as native protein, *upper panel*) was incubated with 50 mM mannitol (*middle panel*) or glucose (*lower panel*) for 48 h, and then subjected to MALDI/MS analysis (see *Materials and Methods*). A representative graph for each condition is reported.

according to previous studies (38) with excitation at 290 nm. The maximum was shifted to 347 nm upon glucose addition (Fig. 2B), suggesting a glucose-in-

duced environmental effect onto the FGF-2 molecule. Moreover, difference spectra reported in Fig. 2B showed near doubling of the fluorescence intensity at

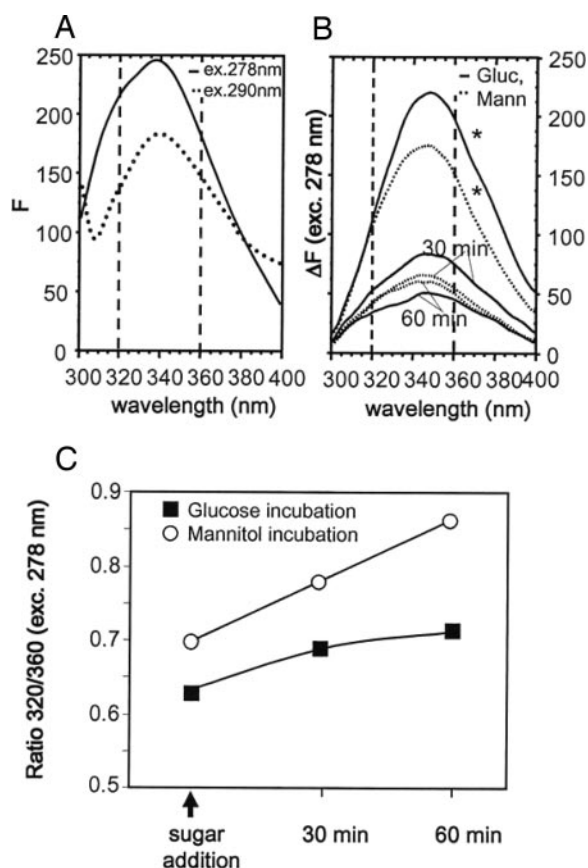


Fig. 2. Structural Analysis: Emission Fluorescence Study
 FGF-2 was incubated with sugars, after which the emission fluorescence scan was recorded and representative spectra are shown. A, FGF-2 fluorescence in the absence of sugars. B, FGF-2 fluorescence in the presence of 50 mM mannitol or glucose. The ordinate axis represents fluorescence excess (ΔF) (see *Materials and Methods*). C, Ratio between intensities at 320 and 360 nm as a function of duration of glucose exposure. ex. or exec., Excitation.

the incubation start (*asterisks*), which thereafter decreased in time. Under these conditions, glucose increased the fluorescence and altered the ratio between intensities at 320 and 360 nm, F_{320}/F_{360} (Fig. 2, B and C), to an extent considerably higher than mannitol, suggesting a marked involvement of tyrosyl and tryptophanyl fluorophores within 60 min exposure to glucose.

FGF-2 is known to require a specific interaction with high-affinity FGF-R1 receptor and a homodimerization step to trigger the signaling cascade (39, 40). Therefore, we investigated whether glucose affects FGF-2 binding and homodimerization properties, under our experimental conditions. Surface plasmonic resonance (SPR) experiments showed that glucose-exposed FGF-2 bound FGF-R1 markedly less than mannitol-exposed FGF-2 (Fig. 3A). Kinetic analyses, performed by evaluating binding features at increasing FGF-2 concentration, indicated that FGF-2 preincubated with glucose binds FGF-R1 with 20-fold less

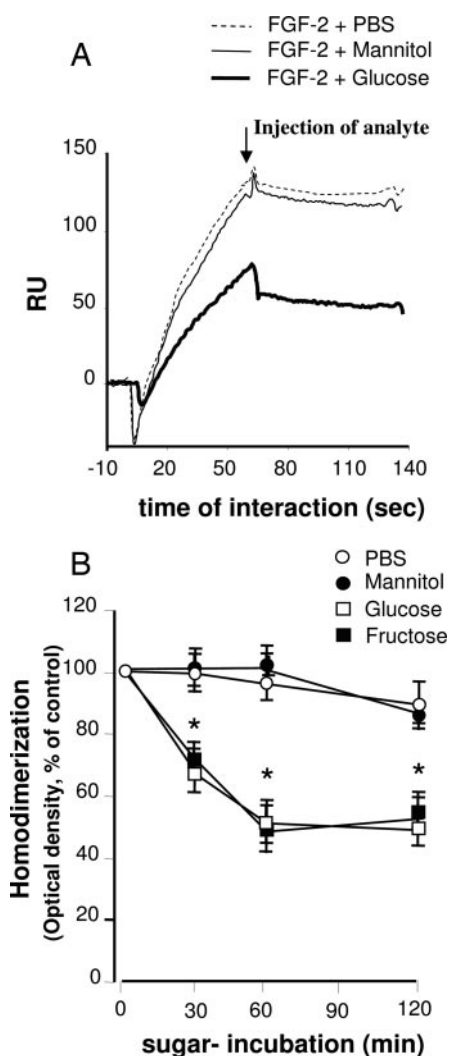


Fig. 3. Binding Analysis
 A, Glucose effects on FGF-2 binding to FGFR1. FGF-2 was treated with mannitol or glucose (50 mM, 1 h), after which its ability to interact with immobilized FGFR-chip was assayed by SPR. Representative sensorgrams are reported. The experiment was carried out three times with similar results. B, FGF-2 homodimerization in the presence of glucose. The effects of glucose treatment (50 mM) on ability of biotinylated FGF-2 to interact with immobilized FGF-2 were evaluated by streptavidin-HRP detection. Data are expressed as mean \pm sd of one representative experiment performed in triplicate.

affinity, as compared with mannitol-treated FGF-2 (Table 1). Additional experiments were then performed to evaluate whether glucose may interfere with FGF-2 homodimerization. After 60 min incubation with 50 mM glucose or fructose, FGF-2 lost about 50% of its ability to homodimerize (Fig. 3B), whereas 25 mM glucose gave about 30% inhibition (data not shown). This significant reduction of FGF-2's ability to homodimerize was already detectable and significant after 30 min exposure to glucose or fructose, but completely absent with mannitol (Fig. 3B). The effects of glucose on homodimerization are not in conflict with results from

Table 1. Glucose Effect on FGF-2 Binding to FGFR1

Immobilized Ligand	Analyte in Solution	k_a ($M^{-1}sec^{-1}$)	k_d (sec^{-1})	K_D (M)
FGFR1	FGF-2 preincubated with 50 mM mannitol	$(4.2 \pm 4.2) \times 10^5$	$(1.6 \pm 0.4) \times 10^{-3}$	$(3.8 \pm 0.7) \times 10^{-9}$
FGFR1	FGF-2 preincubated with 50 mM glucose	$(5.2 \pm 1.8) \times 10^4$	$(4.1 \pm 0.1) \times 10^{-3}$	$(7.9 \pm 2.7) \times 10^{-8}$

Kinetics analysis was performed as described in *Materials and Methods* and legend to Fig. 3A, using FGFR1-immobilized chip and sugar-treated FGF-2 as analyte, injected at increasing concentrations (see *Materials and Methods*).

SDS-PAGE experiments (Fig. 1A). HMM complexes formation and homodimerization reflect different structural phenomena. In fact, HMM complexes, due to covalent-bonds formation, become evident upon long (12–24 h) sugar exposure, whereas the effect on homodimerization, due to a noncovalent interaction, is evident upon short (30–60 min) sugar exposure. Therefore, the effects on HMM complex formation and impairment of homodimerization should be not directly related.

All together, these data indicate a marked structural modification of FGF-2 and a strong reduction of its binding properties upon 60 min incubation with glucose at concentrations very close to those found in hyperglycemic DM patients.

Characterization of the Glucose-Modified FGF-2

To characterize the observed phenomenon and confirm that FGF-2 undergoes a rapid glycation, the formation of glycation products was investigated. FGF-2, incubated for 0–48 h with glucose, fructose, or mannitol, was evaluated in a competitive ELISA using a specific anti-AGE antibody. Results of these experiments are reported in Fig. 4A. Additional immunoblot analyses to confirm the time-dependent formation of glycation products are reported in Fig. 4B ($P < 0.001$). Interestingly, a significant glycation was observed at 36 h incubation by exposing FGF-2 to an even lower glucose concentration (namely 12.5 mM, frankly within hyperglycemic levels) ($P < 0.001$). The dose-dependent effect of sugars was evaluated by competitive ELISA and reported in Table 2. Fructose was slightly more reactive to induce FGF-2 glycation than glucose, whereas mannitol, as expected, was ineffective in all cases. Incubation of BSA, placental growth factor (PIGF), platelet derived growth factor-BB (PDGF-BB) or FGF-2 (0.1 mg/ml final concentration each) with sugars for 0–24 h (Table 2) showed that only FGF-2 was markedly and significantly modified within 12 h, whereas for PIGF a weak effect was detectable at 24 h. BSA, which is known to be glycated under more extreme conditions (21), and PDGF-BB were not significantly modified at any incubation time. These data indicate that, at 25 mM glucose incubation, a highly specific FGF-2 modification occurs, identified as a glycation product formation.

FGF-2 Mitogenic and Chemotactic Activities Are Rapidly Reduced by Low-Glucose Incubation

The *in vitro* angiogenic activity of FGF-2 was tested on ECs. Both FGF-2-induced proliferation and chemo-

taxis were significantly reduced by glucose exposure; such an effect was time dependent and was already statistically significant after 1 h glucose incubation (Fig. 5, A and B).

To address whether the reduced proliferation observed *in vitro* was due to an increased apoptosis, an

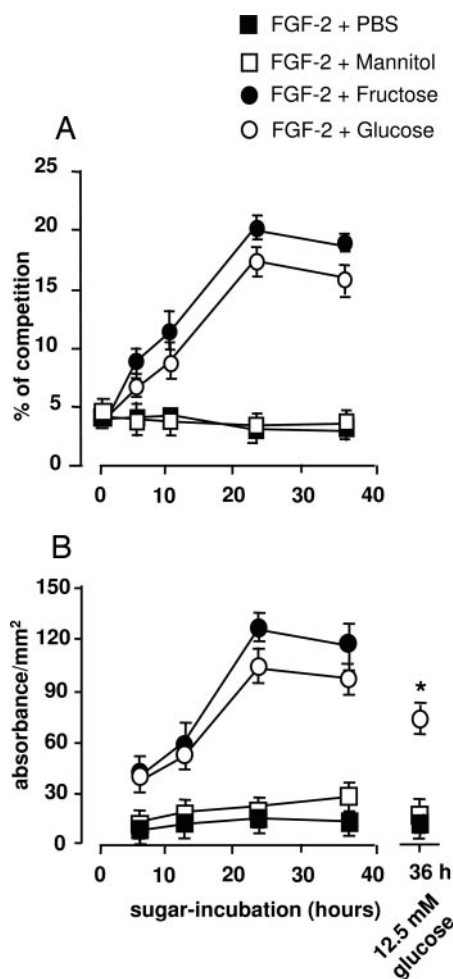


Fig. 4. FGF-2 Glucose-Induced Modification Leads to Glycation Products Formation

A, Competitive ELISA experiments. FGF-2 (11 pmol) was incubated for specified times with 50 mM glucose or control sugars. The 10% competition reported in panel A corresponds to the presence of 5 pmol of glycation product formation. B, Immunoblot analysis: FGF-2 (110 pmol) treated for specified times with PBS, 50 mM or 12.5 mM glucose, or control sugars was blotted onto nitrocellulose and detected with anti-AGE antibody. Immunolabeled dots were quantified by densitometry. Asterisks indicate $P < 0.001$ vs. mannitol.

Table 2. Specificity of Glucose-Induced Glycation by Competitive ELISA Measure

Protein	Incubation with Sugars	Glycation (% of Competition) Mean \pm SD	t Test (<i>P</i> vs. Mannitol)
BSA	0 h Mannitol, 100 mM	5.8 \pm 0.46	—
BSA	0 h Fructose, 100 mM	5.66 \pm 0.71	0.7980
BSA	12 h Mannitol, 100 mM	5.93 \pm 9.21	0.6586
BSA	12 h Fructose, 100 mM	6.1 \pm 0.26	0.4395
BSA	24 h Mannitol, 100 mM	5.76 \pm 0.61	0.7541
BSA	24 h Glucose, 100 mM	6.4 \pm 0.10	0.1511
BSA	24 h Fructose, 100 mM	6.67 \pm 0.42	0.1026
FGF-2	0 h Mannitol, 25 mM	5.57 \pm 0.40	0.7129
FGF-2	0 h Mannitol, 100 mM	5.23 \pm 0.41	0.3695
FGF-2	0 h Glucose, 100 mM	6.03 \pm 0.65	0.1447
FGF-2	0 h Fructose, 100 mM	6.6 \pm 0.61	0.1297
FGF-2	12 h Mannitol, 25 mM	5.47 \pm 0.15	0.8058
FGF-2	12 h Glucose, 25 mM	7.83 \pm 0.85	0.0090
FGF-2	12 h Fructose, 25 mM	8.93 \pm 0.80	0.0018
FGF-2	12 h Glucose, 100 mM	9.17 \pm 0.45	0.0064
FGF-2	12 h Fructose, 100 mM	12.27 \pm 0.76	0.0008
FGF-2	24 h Mannitol, 100 mM	5.9 \pm 0.98	0.8243
FGF-2	24 h Glucose, 100 mM	16.5 \pm 0.9	0.0002
FGF-2	24 h Fructose, 100 mM	20.4 \pm 1.9	0.0002
PDGF-BB	0 h Fructose, 100 mM	5.6 \pm 0.50	0.3791
PDGF-BB	12 h Fructose, 100 mM	6.4 \pm 0.26	0.4436
PDGF-BB	24 h Fructose, 100 mM	6.57 \pm 0.40	0.3390
PIGF	0 h Fructose, 100 mM	5.33 \pm 0.38	0.7700
PIGF	12 h Fructose, 100 mM	7.13 \pm 0.68	0.1489
PIGF	24 h Fructose, 100 mM	8.2 \pm 0.55	0.0254

The specificity of the glucose effect was evaluated by incubation with different proteins and growth factors. Statistically significant values ($P < 0.05$ vs. BSA, 0 h, mannitol 100 mM) are indicated in **bold**. The *dashed line* indicates that Student's *t* test does not apply.

in vitro quantification of programmed cell death was carried out in ECs exposed to FGF-2, pretreated or not with sugars, and compared with controls (Fig. 5C). The results do not show signs of increased apoptosis, compared with controls, indicating that the impaired mitogenic properties of glucose-treated FGF-2 were not due to the activation of an apoptotic pathway.

The phosphorylation of both FGF receptor 1 (FGFR1) and ERK-1/2 induced by FGF-2 (glycated or not) was analyzed in Western blot experiments with anti-phospho-FGFR1 and phospho-Erk-1/2 antibodies. ECs were treated with basal medium without any stimulus (medium alone) or supplemented with fetal calf serum (FCS) or with FGF-2 (unmodified or pre-treated with mannitol or glucose). The glucose-treated FGF-2 (*rightmost* lane in panels of Fig. 5D) was significantly less potent to induce both FGFR1 ($P < 0.01$) and ERK-1/2 ($P < 0.01$) phosphorylation, as compared with mannitol-treated FGF-2 (Fig. 5D), taking the phosphorylation levels back to the basal (*leftmost* lane of Fig. 5D). These results indicate that the glucose-induced modification of FGF-2, under our experimental conditions, markedly impairs its signaling pathway. Further, dose-dependent experiments showed, upon 25 mM glucose exposure, a significant inhibition of FGF-2-induced mitogenic and chemotactic activities, re-

spectively ($P < 0.05$) (Fig. 5, E and F). A significant reduction of both mitogenic and chemotactic activities of FGF-2 exposed to 12.5 mM was also detectable ($P < 0.05$). In both proliferation and chemotaxis assays, glucose was slightly less reactive than fructose. Similar experiments were also carried out on primary human umbilical vein ECs (HUVECs) with similar results (data not shown). These data indicated that fructose and glucose, incubated at low millimolar concentrations and for a short time (*i.e.* 30–60 min) induced a marked loss of chemotactic activity and mitogenic activity of FGF-2.

FGF-2 Glycation Impairs *in Vivo* Angiogenesis

The effect of glucose incubation on the angiogenic properties of FGF-2 was then evaluated *in vivo*. FGF-2 incubated with glucose or mannitol (50 mM) for a specified time was assayed as angiogenic stimulus in chorioallantoic membrane (CAM) assay (Fig. 6A) or mixed with Matrigel and then injected sc in mice. In the latter case, the angiogenic response induced by glucose-incubated FGF-2 was measured in the plugs extracted from mice (Fig. 6B). Exposure to glucose in the CAM assay (30 min) or exposure in the Matrigel-assay (60 min), were sufficient to significantly reduce *in vivo* angiogenic potential of FGF-2 ($P < 0.01$). Glucose and fructose (data not shown) induced similar effects,

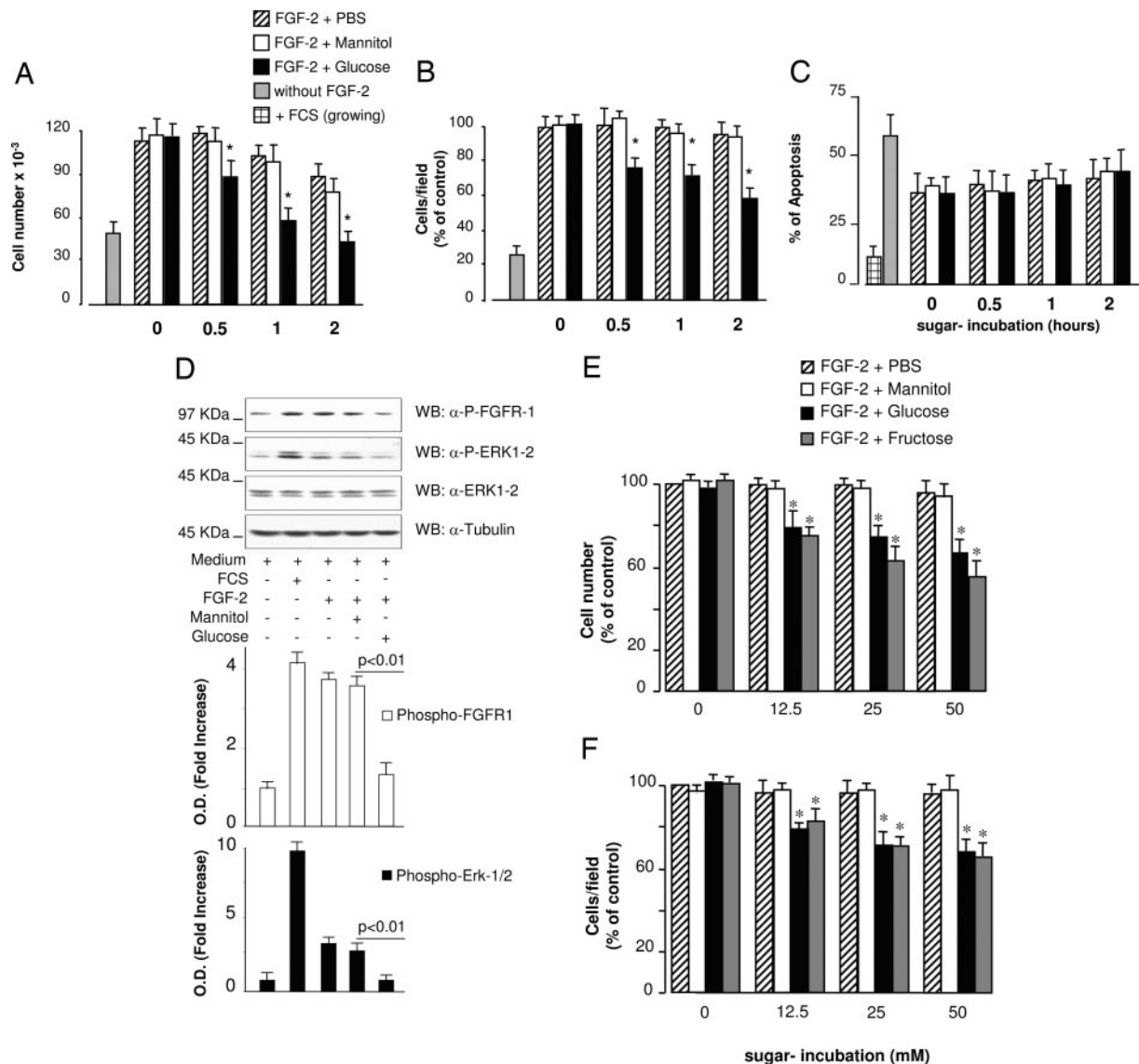


Fig. 5. Effects of Low-Glucose Concentrations on FGF-2-Induced Activity

A, BAEC cells were exposed to FGF-2 preincubated with glucose or control sugars (50 mM) for specified times after which the mitogenic response was compared with mannitol-incubated FGF-2. B, ECs were exposed to FGF-2 preincubated as above and chemotactic response was measured. Cell number in controls (FGF-2 with PBS for 0 h) was $42 \pm 5/\text{field}$. C, ECs were exposed to medium alone (neither serum nor growth factor) or supplemented with FGF-2 preincubated with PBS, glucose, or control sugar (50 mM) as above, or exposed to medium supplemented with FCS, after which the formation of mono- and oligonucleosomes was measured. Data are expressed as a percentage of apoptosis (mean \pm SD of three experiments performed in triplicate). D, FGFR1 and ERK-1/2 phosphorylation in ECs stimulated for 10 min with FGF-2 pretreated with glucose or mannitol (60 min, 50 mM), or under basal (Medium) or FCS-stimulated conditions. Bands of phosphorylated proteins were quantified and normalized by densitometric measures of tubulin bands, expressed as mean \pm SD of one representative experiment performed in triplicate. E and F, Dose-dependent effect of glucose on mitogenic (E) and chemotactic (F) FGF-2 activity was evaluated by using FGF-2 preincubated with sugars for 1 h. Data are expressed as mean \pm SD of three experiments performed in triplicate (*, $P < 0.05$ vs. mannitol). WB, Western blot.

whereas mannitol was not effective. Apoptosis was evaluated on CAMs using terminal deoxynucleotide transferase-mediated deoxyuridine triphosphate nick-end labeling (TUNEL) staining. Sections were studied for the presence of apoptotic cells in the endothelium of blood vessels. No apoptotic ECs were observed (data not shown).

Detection of *in Vivo* Glycated FGF-2

Results reported above prompted us to hypothesize that FGF-2 glycation may occur *in vivo* under hyperglycemic DM conditions; such a hypothesis was then tested in brain extracts from hyperglycemic diabetic mice. Endogenous FGF-2 was analyzed through im-

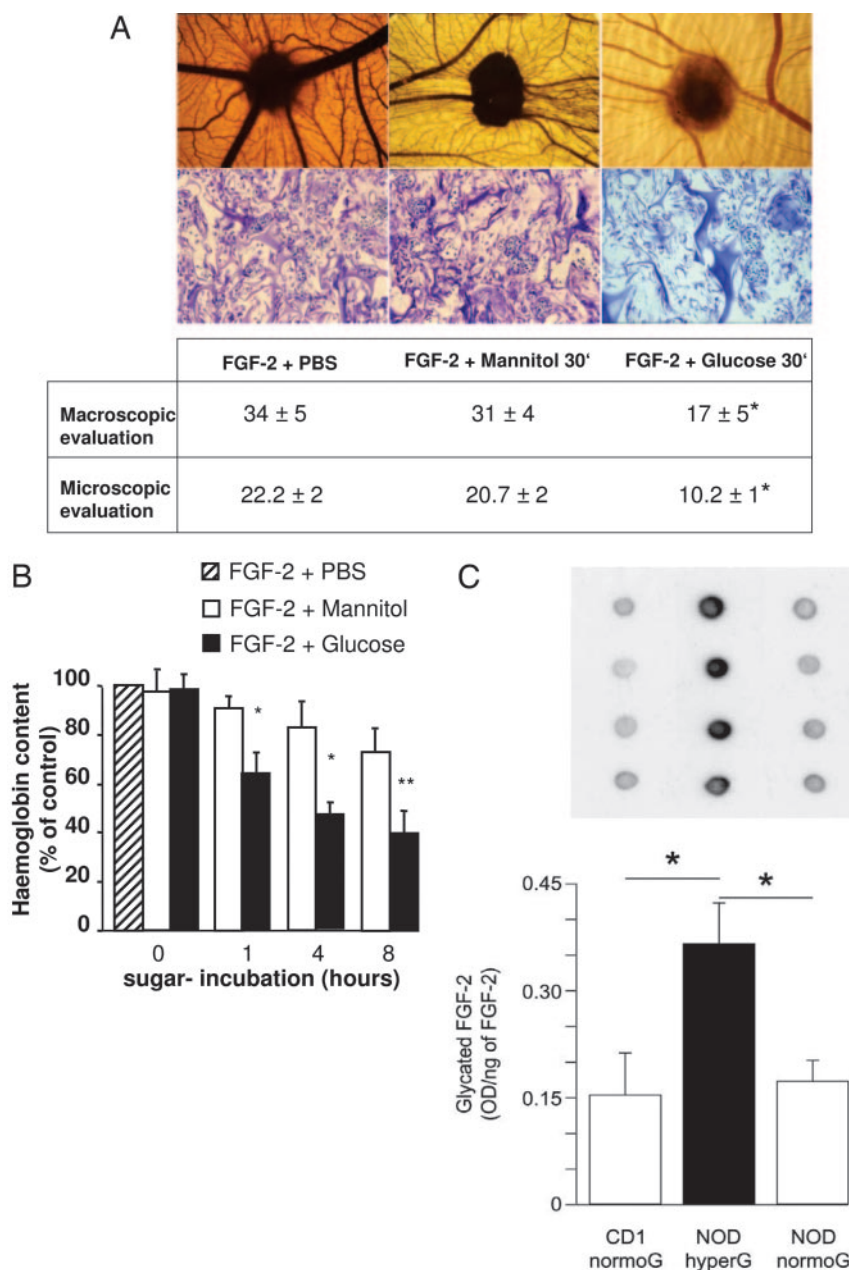


Fig. 6. Glucose Effects on FGF-2-Induced *in Vivo* Angiogenesis and *in Vivo* Glycation of FGF-2

A, Chick embryo CAM-sponge assay: macroscopic and microscopic assessment of vascular density on d 12 of incubation. Macroscopic evaluation represents the number of blood vessels at the sponge-CAM boundary (mean ± SD; magnification, ×50) (*, $P < 0.001$). Microscopic evaluation (magnification, ×250) represents the microvessel density, *i.e.* the percentage of the occupied intersection points referred to their total number of blood vessels inside the sponge. Angiogenic stimulus was FGF-2 incubated with 50 mM glucose or PBS alone. Asterisks indicate the statistical significance ($P < 0.01$) vs. mannitol-incubated FGF-2. B, Matrigel assay in sc tissue of mice: Matrigel was mixed with FGF-2 previously incubated for specified time with mannitol or glucose (50 mM), and then injected in mice (see *Materials and Methods*). Data are reported as percent of angiogenesis measured in control mice (mean ± SD) (*, $P < 0.001$; **, $P < 0.05$ vs. mannitol-treated mice). Hemoglobin content in plugs from mice treated with unmodified FGF-2 was $3.2 \pm 0.2 \mu\text{g}/\text{mg}$ of total protein. C, Glycated-FGF-2 in brain extracts from normoglycemic (CD1-normoG and NOD-normoG) and hyperglycemic (NOD-hyperG) mice ($n = 6$ for each group of mice). Equal amounts of protein extracts have been used for each sample, and total FGF-2 has been measured by a commercial ELISA kit (see *Materials and Methods*). The dot blot analysis from four CD1-normoG, NOD-normoG, and NOD-hyperG mice with the anti-AGE antibody is shown (*upper panel*), and the densitometric analysis is reported (*lower panel*). Asterisks indicate the statistical significance ($P < 0.01$) vs. normoG mice.

munolabeling with anti-AGE antibody, and results from hyperglycemic nonobese diabetic (NOD) mice were compared with normoglycemic mice. Hyperglycemic mice were chosen with average glycemic levels of 28 mM. Brain extracts were chosen because the brain contains a very high FGF-2 concentration. In extracts from hyperglycemic mice, the level of glycated FGF-2 was found to be significantly higher ($P = 0.006$) as compared with extracts from normoglycemic mice (Fig. 6C).

DISCUSSION

In the present study we investigated the glucose effects only, compared with fructose, as an additional reducing sugar, and mannitol as iso-osmotic control, bearing in mind that in serum and tissues from DM patients many other molecules contribute to the total glycation activity. Therefore, the low millimolar concentrations used in the current study may be considered to relate well to hyperglycemic diabetic conditions. Further, previous studies showed that long-term (*i.e.* days or weeks) exposure to high-sugar concentrations may efficiently modify *in vitro* a number of proteins. In the present study, markedly milder conditions (incubation time as short as 30–60 min with glucose concentration as low as 12.5 mM) were sufficient to induce the formation of an FGF-2 glycated product and to induce significant modifications of FGF-2 structure and function, both *in vitro* and *in vivo*. It is noteworthy that the antibody used to detect the glycated FGF-2-product was specifically developed to recognize early- or intermediate-AGE products: in the present study it recognized more efficiently the FGF-2 produced at short incubation time, as compared with longer incubations (see Fig. 4, time point at 36 h), possibly suggesting the formation of an early or intermediate glycation product of FGF-2 under these experimental conditions. Recently published studies showed that another antibody raised against a similar antigen was able to prevent experimental diabetic retinopathy (41), confirming a potential role of similar glycation products in development of DM vascular complications and suggesting novel potential therapeutic approaches.

It is noteworthy that 1-h glucose incubation induced the formation of an FGF-2 glycated product concomitantly with the changes of FGF-2 fluorescence. In experiments reported in Fig. 2, glucose addition caused a red shift of the maximum intensity from 340–347 nm, suggesting a major structural modification (compare Fig. 2, A and B). The glucose effect is better appreciated by the F_{320}/F_{360} ratio, which estimates changes in shape of the spectrum. In fact, upon sugar addition, it was invariably lower than 1 and significantly lower for glucose than for mannitol, more markedly at 60 min of incubation, indicating the occurrence of glucose-induced FGF-2 structural modifications

(Fig. 2C). It is noteworthy that 60 min exposure of FGF-2 to 50 mM glucose determines 1) a significant reduction (50%) of FGF-2 homodimerization (necessary step for FGF-2 to exert its biological activity), 2) a strong reduction (>20-fold) in binding affinity to FGFR1, and 3) a 56% reduction of Erk-1/2 phosphorylation in HUVECs. Therefore, it is reasonable to hypothesize that hyperglycemia may impair FGF-2 homodimerization, FGF-2 binding to its receptor, and activation of the signal transduction pathway, with a subsequent significant loss of *in vitro* and *in vivo* angiogenic properties (~50% inhibition of proliferation and migration features). To rule out that the reduced proliferation observed in our *in vitro* system was not due to the activation of an apoptotic pathway, a direct quantification of apoptosis was carried out by a photometric ELISA. ECs were exposed to FGF-2 treated or not with sugars and compared with controls. The results from these experiments *in vitro* confirmed that the impaired mitogenic properties of glucose-treated FGF-2 were not due to the activation of an apoptotic pathway. Further, *in vivo* apoptosis was evaluated on CAMs using TUNEL staining. Sections were studied for the presence of apoptotic cells in the endothelium of blood vessels. Under the present experimental conditions no apoptotic cells were observed (data not shown), indicating that the impairment of FGF-2 angiogenic features was not due to an apoptosis increase. However, the possibility cannot be ruled out that glycated-FGF-2 may impair angiogenesis through the activation of an apoptotic pathway in another *in vivo* model. Mass spectrometry and biochemical and functional analyses carried out in the present study represent the first direct evidence of the formation of glucose adduct in FGF-2 molecule, possibly due to glycation, upon experimental conditions comparable to hyperglycemia. An inverse correlation between glycemic level and exogenous-FGF-2-induced angiogenesis in NOD mice is known (16); in the present study, for the first time, the direct evidence of *in vivo* glycation of endogenous FGF-2 has been reported in tissues of hyperglycemic NOD mice with glycemic levels (28 mM in average) very close to the glucose levels used throughout the analyses carried out in the current study. Glycation of endogenous FGF-2 was significantly less evident both in CD1 and in normoglycemic NOD mice, indicating that endogenous FGF-2 glycation was likely related to the hyperglycemic status. These results confirm that this glucose-induced modification of FGF-2 occurs *in vivo* and strongly support this as a novel and specific mechanism underlying the angiogenesis impairment in DM patients.

In conclusion, the present study suggests a novel role of protein glycation to control structural and functional features of specific regulatory angiogenic proteins exposed to hyperglycemia and may open interesting new perspectives to study the effects of glucose not only in pathological but also in physiological conditions.

MATERIALS AND METHODS

Experimental Animals

Procedures involving animals and their care were conducted in conformity with institutional guidelines in compliance with international laws and policies (NIH Guide for the Care and Use of Laboratory Animals, 1996).

Materials

Human recombinant FGF-2, human recombinant PIGF and human recombinant PDGF-BB were from R&D Systems, Inc. (Minneapolis, MN). The FGFR-Fc chimera used for binding studies was from R&D. The Biacore X instrument (Biacore AB, Uppsala, Sweden), sensor chips CM5, surfactant P20, and the amine-coupling kit containing N-hydroxysuccinimide, N-ethyl-N'-(3-diethylaminopropyl) carbodiimide, and ethanolamine hydrochloride were from Pharmacia Biosensor AB (Amersham Pharmacia Biotech, Uppsala, Sweden). The anti-PDGF-BB and anti-FGF-2 antibodies were from R&D. Chemicals for immunoblot and western Blot analysis were from Amersham Pharmacia Biotech and Santa Cruz Biotechnology, Inc. (Santa Cruz, CA). ELISA kits for FGF-2 quantification were from R&D. All other reagents were of the highest purity available and were purchased from Sigma Chemical Co. (St. Louis, MO).

Glucose-Dependent Modification of FGF-2 and Other Proteins

Human recombinant FGF-2 was dissolved in glycation buffer solution (0.9% NaCl, 0.144 g/liter KH_2PO_4 , 0.426 g/liter Na_2HPO_4) pH 7.4, at 10 $\mu\text{g}/\text{ml}$ final concentration and immediately frozen at -80°C , under sterile conditions, after which FGF-2 aliquots were incubated at 37°C for different times (from 0–48 h in sealed vials) with different concentrations of glucose, fructose, or mannitol. These samples were then diluted at least 1000 times to be tested in functional assays. FGF-2 incubated with glucose was also subjected to Western blot (not shown), immunoblotting (through Dot Blot assay) and competitive ELISA using a polyclonal anti-AGE antibody (see below) and detected via a chemiluminescent detection assay (ECL, Amersham Pharmacia). SDS-PAGE and radiolabeling studies with D-[1- ^{14}C]-glucose were carried out as described (16). Nonspecific binding of glycated proteins to plastics was minimized by careful handling and evaluation of protein recovery after each manipulation.

Data reported in competitive ELISA, SDS-PAGE, and immunoblot analyses were carried out at least three times, with similar results.

Matrix-Assisted Laser Desorption Ionization Mass Spectrometry (MALDI/MS)

FGF-2 samples, after incubation with glucose or mannitol at the specified doses, were analyzed by MALDI/MS on a Voyager DE-Pro mass spectrometer (Applied Biosystems, Foster City, CA) operating in positive-ion linear mode. A mixture of analyte solution and saturated solution of sinapinic acid (10 mg/ml in acetonitrile/0.2% trifluoroacetic acid 40:60) (Sigma) was applied to the metallic sample plate and dried. Average mass values were measured in this analysis. The instrument was calibrated using a standard mixture of proteins provided by the manufacturer and following their procedures. FGF-2 fragments were generated using a cyanogen bromide treatment, according to a published protocol (37).

Competitive ELISA

The rabbit AGE-RNase polyclonal antibody used in this study was developed against RNase incubated for 20 d with 25 mM methyl glyoxal (Fluka, Buchs, Switzerland). Hyperimmune serum was obtained according to standard protocols and stored at -80°C until use. The antiserum was characterized by Western blot and competitive ELISA studies, as previously described (16). Briefly, anti-AGE antibody was assayed against BSA, ovalbumin, and casein, obtained by incubation with 250 mM fructose for 7 d, or β -lactoglobulin incubated with 250 mM methyl glyoxal for 7 d. To determine FGF-2 sugar-induced modification, 96-well flexible ELISA plates were coated with 10 $\mu\text{g}/\text{ml}$ glycated-BSA (*i.e.* preincubated with methyl glyoxal as above) and incubated at 4°C overnight. After blocking with 10% horse serum, 0.1 ml aliquots of rabbit antiserum (1:4000), in the presence of glycated FGF-2, were added at 37°C for 1 h. Peroxidase-conjugated anti-rabbit IgG secondary antibodies and tetramethylbenzidine (Bio-Rad Laboratories, Inc., Hercules, CA) were used for a colorimetric assay measuring OD at 450 nm.

Fluorescence Studies

Fluorescence studies were carried out as reported elsewhere (42). FGF-2 (10 $\mu\text{g}/100 \mu\text{l}$ final volume in glycation buffer solution) was incubated at 37°C in the presence and the absence of mannitol or glucose, and steady-state fluorescence emission spectra were collected at regular time intervals with a PerkinElmer LS55 instrument (PerkinElmer, Inc., Boston, MA), using an excitation wavelength of 278 nm, equal bandwidths for excitation and emission, 120 nm/min scan speed, and 1-sec integration time. Final spectra of glucose-incubated FGF-2 were obtained after subtraction of the separate contributions of protein and each sugar. Fluorescence excess (ΔF) was obtained by subtracting contributions from separate FGF-2 and sugar solutions from the fluorescence of the sugar/FGF-2 mixture assayed.

SPR Studies

FGF-2 binding studies were carried out on a Biacore X instrument according to previously reported procedures (42). To study FGFR/FGF-2 interaction, protein A (70 μl , 300 $\mu\text{g}/\text{ml}$) diluted in 30 mM acetate buffer, pH 4.2, was covalently coupled to a CM5 sensor chip according to a published procedure (43). The FGFR1 extracellular domain, fused to the mouse heavy chain IgG2a (FGFR-Fc), was then immobilized [~ 1000 resonance units (RU)]. Human recombinant FGF-2 (20 μl , 150 nM, 3 $\mu\text{g}/\text{ml}$), previously incubated in the presence or in the absence of 50 mM glucose, fructose, or mannitol (37°C for different times), was injected on FGFR-Fc-coated sensor chip for 2 min association phase and 30 sec dissociation phase. The response expressed in RU was monitored at 25°C and reported upon subtraction of the reference cell, to subtract bulk refractive index background and nonspecific binding. Sensor chip regeneration was successfully achieved by 10 μl of 50 mM NaOH injection.

In additional experiments, different concentrations of FGF-2 (in the range of 0–1200 nM) were preincubated with 50 mM glucose at 37°C for 60 min for kinetics evaluation, according to previously published procedures (44).

Kinetic Data Analysis

Biacore sensorgrams were analyzed by nonlinear least squares curve fitting using the BIAevaluation software version 3.0 (Biacore Pharmacia). Kinetic constants were generated from the association and dissociation curves from the SPR experiments by fitting to a single-site binding model (Langmuir model: $A + B = AB$), as previously reported (42).

The apparent equilibrium dissociation constant, k_d , was computed as the ratio of these kinetic constants (45, 46). This model computed a single exponential fit with a $\chi^2 < 0.5$. The equation

$$R_t = R_0 \exp[-k_d(t - t_0)]$$

was used for the dissociation phase, where R_t is the amount of bound ligand expressed in RU at time t and t_0 is the beginning of dissociation phase. The final dissociation rate constant, k_d , was calculated from the mean values obtained from injections performed at least in duplicate. To analyze the association phase, the equation

$$Rt = R_{eq}(1 - \exp(-k_s(t - t_0)))$$

was employed, where R_{eq} is the amount of bound ligand (expressed in RU) at equilibrium, t_0 is the starting time of injection, and

$$k_s = k_a C + k_d$$

where C is the concentration of analyte injected over the sensor chip surface. The association rate constant, k_a , was determined as the slope of a plot of k_s vs. C . The apparent equilibrium dissociation constant, K_D , was determined as the ratio of these two kinetic constants (45, 46)

$$K_D = k_d/k_a$$

FGF-2 Homodimerization

FGF-2 was diluted in assay buffer AC7.5 (50 mM Tris-HCl, pH 7.5; 100 mM KCl; 3 mM MgCl₂; 1 mM CaCl₂) at 7 μ g/ml final concentration; then 100 μ l/well solution was incubated at 4 C for 4 h in microplate (Costar, Cambridge, MA) and subsequently blocked with 300 μ l/well of 30 mg/ml BSA (Sigma) diluted in AC7.5 for 16 h at 4 C. The next day, biotinylated FGF-2 was diluted in AC7.5T-BSA buffer (AC7.5 buffer added with 0.1% Tween 20 and 0.15 mg/ml BSA; Sigma) and dispensed onto FGF-2-coated wells, for 3 h at room temperature. Unbound material was then washed out and wells were incubated for 60 min with AB complex (Vecstatine, Vector Laboratories, Burlingame, CA) conjugated with alkaline phosphatase (100 μ l/well). Plates were washed once with AC7.5T-BSA and twice with diethanolamine buffer (10 mM diethanolamine, 0.5 mM MgCl₂), incubated with *p*-nitrophenyl phosphate (pNPP) in diethanolamine buffer (100 μ l/well), and the colorimetric reaction was detected at 405 nm according to the manufacturer's instructions using an ELISA plate reader spectrophotometer (Bio-Rad).

Primary Cultures of ECs

Primary bovine aorta ECs (BAECs) and primary HUVECs were prepared and cultured as described (47). Culture purity was consistently more than 98% according to cobblestone arrangement and to Dil-Ac-LDL uptake. BAECs were maintained in DMEM supplemented with 10% FCS (Euroclone Ltd., Paignton, UK), 2 mM γ -glutamine, and 100 IU/ml penicillin/streptomycin (GIBCO, Paisley, UK) in humidified 5% CO₂ atmosphere at 37 C. All experiments were performed with cells at passage 2–6.

In Vitro Migration and Proliferation Studies

Migration assays with BAECs (2×10^5) were carried out in modified Boyden chambers (Costar Scientific Corp., Cambridge, MA) as described (47). Glucose-incubated human recombinant FGF-2 (10 ng/ml) was used as chemoattractant, in the lower portion of a Boyden chamber. Assays were carried out at 37 C in 5% CO₂ humidified incubators, for 6 h. Migrated cells were counted at $\times 400$ magnification; 10 fields/filter were evaluated, and the average number of cells per field was reported. In proliferation assays, ECs plated in six-well plates (1×10^5 cells per plate) were grown for 24 h

in DMEM (for BAECs) or EBM-2 (for HUVECs) supplemented with 10% FCS or EGM-2 kit (respectively) at 37 C in 5% CO₂. Medium was then replaced with a serum-free medium, for 24 h. Subsequently, the medium was replaced with fresh medium containing either 0.1% BSA alone or 0.1% BSA supplemented with growth factors previously incubated with sugars. After 48 h treatment, cells were harvested and counted with a hemacytometer. All experiments were carried out at least three times in duplicate, with similar results.

In Vitro Assessment of Apoptosis

In vitro apoptosis was measured by photometric enzyme immunoassay (Cell Death Detection ELISA; Roche Clinical Laboratories, Indianapolis, IN), to quantify cytoplasmic histone-associated DNA fragments (mono- and oligonucleosomes) as previously described (47).

FGFR1 and MAPK Activation Study

FGFR1 and ERK-1/2 phosphorylation was detected in extracts from ECs exposed for 10 min to FGF-2 treated with 50 mM glucose or mannitol as control, using anti-phospho-FGFR1 (Abgent, San Diego, CA) and anti-ERK-1/2 and anti-phospho-Erk-1/2 (Cell Signaling Technology, Inc., Beverly, MA) antibodies according to a published protocol (48). Equal amounts of total proteins (100 μ g/lane) were electrophoresed in 12% SDS-PAGE under reducing conditions and electroblotted to a nitrocellulose membrane Optitran BA-S 83 (Schleicher & Schuell, Keene, NH). Proteins were detected by incubating the membrane with specific antibodies according to manufacturer's instructions and evidenced by incubation with a secondary peroxidase-conjugated antibody and ECL detection system (Amersham Pharmacia Biotech), according to manufacturer's instructions. Loading of equal amount of total proteins and normalization were assessed by densitometric measures of tubulin bands.

In Vivo Studies

Angiogenesis Matrigel Assay. Angiogenesis in reconstituted basement membrane (Matrigel; Becton Dickinson and Co., Franklin Lakes, NJ) plugs was evaluated as reported (49). Matrigel added with FGF-2 (150 ng/ml) or added with sugar-incubated FGF-2 (50 mM glucose or mannitol as control) was injected sc in C57BL/6 female mice, 10 mice per group, 15–16 wk of age (Charles River Laboratories, Wilmington, MA) (16). Mice were housed under controlled temperature (23 C) and lighting, with free access to water and standard mouse chow. Mice were killed 8 d after injection and Matrigel plugs were excised and included in paraffin: plugs with evident blood extravasation were excluded by the analysis. Angiogenesis was quantified according to hemoglobin content, as described (49) after normalization for total protein content.

CAM Assay. The CAM assay was performed according to a published procedure (50). Fertilized White Leghorn chicken eggs were incubated at 37 C at constant humidity. On d 3 of incubation a square window was opened in the egg shell after removal of 2–3 ml of albumin to detach the developing CAM from the shell. The window was sealed with a glass and the eggs were returned to the incubator. On d 8, 1 mm³ sterilized gelatin sponges (Gelfoam; Upjohn, Kalamazoo, MI) were placed on the top of the growing CAM. The sponges were loaded with 2 μ l of PBS containing 500 ng of recombinant human FGF-2 (GIBCO) only, or FGF-2 incubated at 37 C for 30 min with 50 mM glucose or mannitol. CAMs were examined daily until d 12 and photographed *in ovo* with a stereomicroscope equipped with a Camera System MC 63 (Zeiss, Oberkochen, Germany). On d 12, blood vessels entering the sponges or the implants within the focal plane of

the CAM were counted by two observers in a double-blind fashion at $\times 50$ magnification. Mean values \pm SD of vessel counts were determined for each analysis. Finally, CAMs were fixed *in ovo* in Bouin's fluid, dehydrated in graded ethanol, embedded in paraffin, serially sectioned at 7 μ m, according to a plane perpendicular to their free surface, and stained with a 0.5% aqueous solution of Toluidine blue (Merck, Darmstadt, Germany). The angiogenic response was assessed histologically by a planimetric method of point counting (50). The vascular density was indicated as a percentage of the occupied intersection points referred to their total number. Apoptotic cells were stained using the Terminal deoxynucleotide transferase-mediated deoxyuridine triphosphate nick-end labeling (TUNEL) technique, according to a published report (15).

***In Vivo* Glycation of FGF-2.** Brain extracts were prepared as described previously (51) from control CD1 mice (six females 16–21 wk of age; mean blood glucose = 88 ± 12 mg/100 ml), normoglycemic NOD/Ltj mice (Charles River; six females 12–21 wk of age; mean blood glucose = 95 ± 14 mg/100 ml) and hyperglycemic NOD/Ltj mice (Charles River; six females 16–21 wk of age; mean blood glucose = 498 ± 142 mg/100 ml, corresponding to 28 mm, on the average). Mice maintenance and glycemic measurements were performed as described elsewhere (16). A monoclonal antibody to FGF-2 (R&D) was spotted onto nitrocellulose (antibody diluted at 10 μ g/ml in PBS-BSA 1%, four spots of 10 μ l for each mouse brain extract), after which 30 mg of total proteins from each postnuclear supernatant (*i.e.* 10 ml of brain extract with 3 mg/ml protein concentration) was incubated onto the nitrocellulose for 2 h at room temperature. These experiments were carried out with a monoclonal anti-FGF-2 (R&D), the same used to immobilize onto ELISA plates FGF-2 from serum, cell lysates, and tissue homogenates. Therefore it was assumed that such antibody spotted onto the nitrocellulose would bind with good affinity and specificity the FGF-2 present in brain lysates. After four washes with PBS-Tween, membranes were hybridized with anti-AGE polyclonal antibody (1:4,000, 2 h, RT), washed, and incubated with HRP-antirabbit IgG-conjugated antibody (1:10,000); signal was then measured by ECL followed by densitometry analysis. For normalization, brain extracts were previously assayed for total protein concentration, and extracts were diluted to obtain the same total protein concentration, after which the ECL signal detected by the anti-AGE antibody was reported as referred to the total FGF-2 content measured by ELISA (R&D) (OD/ng of FGF-2).

Statistical Analysis

Data were expressed as mean \pm SD. All experiments were performed at least three times. Student's two-tailed *t* test was performed and a $P \leq 0.05$ was considered statistically significant.

Acknowledgments

Received August 4, 2005. Accepted July 6, 2006.

Address all correspondence and requests for reprints to: Francesco Facchiano, M.D., Dipartimento di Ematologia, Oncologia e Medicina Molecolare, Istituto Superiore di Sanità, Viale Regina Elena 299, 00161 Roma, Italy. E-mail: facchiano@iss.it.

This work was supported by Telethon-Italy (Grant 1167) and by Istituto Superiore di Sanità-Italy "Programma Nazionale Cellule Staminali" (to F.F.).

Disclosure Statement: all authors (F.F., D.D., K.R., V.F., C.M., R.R., G.Z., V.C., D.R., C.P., M.C.C., A.F.) have nothing to declare.

REFERENCES

- Aronson D 2003 Cross-linking of glycated collagen in the pathogenesis of arterial and myocardial stiffening of aging and diabetes. *J Hypertens* 21:3–12
- Stehbens WE 1990 The epidemiological relationship of hypercholesterolemia, hypertension, diabetes mellitus and obesity to coronary heart disease and atherogenesis. *J Clin Epidemiol* 43:733–741
- Chettab K, Zibara K, Belaiba SR, McGregor JL 2002 Acute hyperglycaemia induces changes in the transcription levels of 4 major genes in human endothelial cells: macroarrays-based expression analysis. *Thromb Haemost* 87:141–148
- Laakso M 1999 Hyperglycemia and cardiovascular disease in type 2 diabetes. *Diabetes* 48:937–942
- Di Carli MF, Janisse J, Grunberger G, Ager J 2003 Role of chronic hyperglycemia in the pathogenesis of coronary microvascular dysfunction in diabetes. *J Am Coll Cardiol* 41:1387–1393
- Shaw JE, Boulton AJ 1997 The pathogenesis of diabetic foot problems: an overview. *Diabetes* 46(Suppl 2):S58–S61
- Wautier JL, Schmidt AM 2004 Protein glycation: a firm link to endothelial cell dysfunction. *Circ Res* 95:233–238
- Jakus V, Rietbrock N 2004 Advanced glycation end-products and the progress of diabetic vascular complications. *Physiol Res* 53:131–142
- Aso Y, Inukai T, Tayama K, Takemura Y 2000 Serum concentrations of advanced glycation endproducts are associated with the development of atherosclerosis as well as diabetic microangiopathy in patients with type 2 diabetes. *Acta Diabetol* 37:87–92
- Phillips SA, Thornalley PJ 1993 The formation of methylglyoxal from triose phosphates. Investigation using a specific assay for methylglyoxal. *Eur J Biochem* 212:101–105
- Yaylayan VA, Keyhani A 2001 Carbohydrate and amino acid degradation pathways in L-methionine/D- 13 C] glucose model systems. *J Agric Food Chem* 49:800–803
- Richard JP 1991 Kinetic parameters for the elimination reaction catalyzed by triosephosphate isomerase and an estimation of the reaction's physiological significance. *Biochemistry* 30:4581–4585
- Glomb MA, Monnier VM 1995 Mechanism of protein modification by glyoxal and glycolaldehyde, reactive intermediates of the Maillard reaction. *J Biol Chem* 270:10017–10026
- Loidl-Stahlhofen A, Hannemann K, Spiteller G 1994 Generation of α -hydroxyaldehydic compounds in the course of lipid peroxidation. *Biochim Biophys Acta* 1213:140–148
- Larger E, Marre M, Corvol P, Gasc JM 2004 Hyperglycemia-induced defects in angiogenesis in the chicken chorioallantoic membrane model. *Diabetes* 53:752–761
- Facchiano F, Lentini A, Fogliano V, Mancarella S, Rossi C, Facchiano A, Capogrossi MC 2002 Sugar-induced modification of fibroblast growth factor 2 reduces its angiogenic activity *in vivo*. *Am J Pathol* 161:531–541
- Abaci A, Oguzhan A, Kahraman S, Eryol NK, Unal S, Arinc H, Ergin A 1999 Effect of diabetes mellitus on formation of coronary collateral vessels. *Circulation* 99:2239–2242
- Rivard A, Silver M, Chen D, Kearney M, Magner M, Annex B, Peters K, Isner JM 1999 Rescue of diabetes-related impairment of angiogenesis by intramuscular gene therapy with adeno-VEGF. *Am J Pathol* 154:355–363
- Ahmed MU, Thorpe SR, Baynes JW 1986 Identification of N ϵ -carboxymethyllysine as a degradation product of fructoselysine in glycated protein. *J Biol Chem* 261:4889–4894

20. Fu MX, Knecht KJ, Thorpe SR, Baynes JW 1992 Role of oxygen in cross-linking and chemical modification of collagen by glucose. *Diabetes* 41(Suppl 2):42–48
21. Coussons PJ, Jacoby J, McKay A, Kelly SM, Price NC, Hunt JV 1997 Glucose modification of human serum albumin: a structural study. *Free Radic Biol Med* 22:1217–1227
22. Facchiano F, Libondi T, Stiuso P, Esposito C, Ragone R, Colonna G 1996 Effect of galactose on α -crystallin. *Ophthalmic Res* 28(Suppl 1):97–100
23. Dyer DG, Dunn JA, Thorpe SR, Bailie KE, Lyons TJ, McCance DR, Baynes JW 1993 Accumulation of Maillard reaction products in skin collagen in diabetes and aging. *J Clin Invest* 91:2463–2469
24. Lyons TJ, Silvestri G, Dunn JA, Dyer DG, Baynes JW 1991 Role of glycation in modification of lens crystallins in diabetic and nondiabetic senile cataracts. *Diabetes* 40:1010–1015
25. Aronson D, Rayfield EJ 2002 How hyperglycemia promotes atherosclerosis: molecular mechanisms. *Cardiovasc Diabetol* 1:1
26. Berg TJ, Clausen JT, Torjesen PA, Dahl-Jorgensen K, Bangstad HJ, Hanssen KF 1998 The advanced glycation end product N ϵ -(carboxymethyl)lysine is increased in serum from children and adolescents with type 1 diabetes. *Diabetes Care* 21:1997–2002
27. Ruderman NB, Williamson JR, Brownlee M 1992 Glucose and diabetic vascular disease. *FASEB J* 6:2905–2914
28. Schleicher ED, Wagner E, Nerlich AG 1997 Increased accumulation of the glycoxidation product N ϵ -(carboxymethyl)lysine in human tissues in diabetes and aging. *J Clin Invest* 99:457–468
29. Soulis T, Thallas V, Youssef S, Gilbert RE, McWilliam BG, Murray-McIntosh RP, Cooper ME 1997 Advanced glycation end products and their receptors co-localise in rat organs susceptible to diabetic microvascular injury. *Diabetologia* 40:619–628
30. Vlassara H, Bucala R, Striker L 1994 Pathogenic effects of advanced glycosylation: biochemical, biologic, and clinical implications for diabetes and aging. *Lab Invest* 70:138–151
31. Makita Z, Vlassara H, Cerami A, Bucala R 1992 Immunohistochemical detection of advanced glycosylation end products *in vivo*. *J Biol Chem* 267:5133–5138
32. Brownlee M, Cerami A, Vlassara H 1988 Advanced glycosylation end products in tissue and the biochemical basis of diabetic complications. *N Engl J Med* 318:1315–1321
33. Yeboah FK, Alli I, Yaylayan VA, Yasuo K, Chowdhury SF, Purisima EO 2004 Effect of limited solid-state glycation on the conformation of lysozyme by ESI-MS/MS peptide mapping and molecular modeling. *Bioconjug Chem* 15:27–34
34. Winlove CP, Parker KH, Avery NC, Bailey AJ 1996 Interactions of elastin and aorta with sugars *in vitro* and their effects on biochemical and physical properties. *Diabetologia* 39:1131–1139
35. Rosenthal NR, Barrett EJ 1985 An assessment of insulin action in hyperosmolar hyperglycemic nonketotic diabetic patients. *J Clin Endocrinol Metab* 60:607–610
36. Sun Y, Hayakawa S, Izumori K 2004 Modification of ovalbumin with a rare ketohexose through the Maillard reaction: effect on protein structure and gel properties. *J Agric Food Chem* 52:1293–1299
37. Minetti M, Pietraforte D, Carbone V, Salzano AM, Scorza G, Marino G 2000 Scavenging of peroxynitrite by oxyhemoglobin and identification of modified globin residues. *Biochemistry* 39:6689–6697
38. Burgermeister J, Paper DH, Vogl H, Linhardt RJ, Franz G 2002 LaPSvS1, a (1 \rightarrow 3)- β -galactan sulfate and its effect on angiogenesis *in vivo* and *in vitro*. *Carbohydr Res* 337:1459–1466
39. Facchiano A, Russo K, Facchiano AM, De Marchis F, Facchiano F, Ribatti D, Aguzzi MS, Capogrossi MC 2003 Identification of a novel domain of fibroblast growth factor 2 controlling its angiogenic properties. *J Biol Chem* 278:8751–8760
40. Perollet C, Han ZC, Savona C, Caen JP, Bikfalvi A 1998 Platelet factor 4 modulates fibroblast growth factor 2 (FGF-2) activity and inhibits FGF-2 dimerization. *Blood* 91:3289–3299
41. Hammes HP, Du X, Edelstein D, Taguchi T, Matsumura T, Ju Q, Lin J, Bierhaus A, Nawroth P, Hannak D, Neumaier M, Bergfeld R, Giardino I, Brownlee M 2003 Benfotiamine blocks three major pathways of hyperglycemic damage and prevents experimental diabetic retinopathy. *Nat Med* 9:294–299
42. Russo K, Ragone R, Facchiano AM, Capogrossi MC, Facchiano A 2002 Platelet-derived growth factor-BB and basic fibroblast growth factor directly interact *in vitro* with high affinity. *J Biol Chem* 277:1284–1291
43. Goretzki L, Burg MA, Grako KA, Stallcup WB 1999 High-affinity binding of basic fibroblast growth factor and platelet-derived growth factor-AA to the core protein of the NG2 proteoglycan. *J Biol Chem* 274:16831–16837
44. Bailly S, Brand C, Chambaz EM, Feige JJ 1997 Analysis of small latent transforming growth factor- β complex formation and dissociation by surface plasmon resonance. Absence of direct interaction with thrombospondins. *J Biol Chem* 272:16329–16334
45. Herzog A, Szegedi C, Jona I, Herberg FW, Varsanyi M 2000 Surface plasmon resonance studies prove the interaction of skeletal muscle sarcoplasmic reticular Ca(2+) release channel/ryanodine receptor with calsequestrin. *FEBS Lett* 472:73–77
46. Newbell BJ, Anderson JT, Jarrett HW 1997 Ca²⁺-calmodulin binding to mouse α 1 syntrophin: syntrophin is also a Ca²⁺-binding protein. *Biochemistry* 36:1295–1305
47. D'Arcangelo D, Facchiano F, Barlucchi LM, Melillo G, Illi B, Testolin L, Gaetano C, Capogrossi MC 2000 Acidosis inhibits endothelial cell apoptosis and function and induces basic fibroblast growth factor and vascular endothelial growth factor expression. *Circ Res* 86:312–318
48. De Marchis F, Ribatti D, Giampietri C, Lentini A, Faraone D, Scoccianti M, Capogrossi MC, Facchiano A 2002 Platelet-derived growth factor inhibits basic fibroblast growth factor angiogenic properties *in vitro* and *in vivo* through its α receptor. *Blood* 99:2045–2053
49. McMahon GA, Petitclerc E, Stefansson S, Smith E, Wong MK, Westrick RJ, Ginsburg D, Brooks PC, Lawrence DA 2001 Plasminogen activator inhibitor-1 regulates tumor growth and angiogenesis. *J Biol Chem* 276:33964–33968
50. Ribatti D, Gualandris A, Bastaki M, Vacca A, Iurlaro M, Roncali L, Presta M 1997 New model for the study of angiogenesis and antiangiogenesis in the chick embryo chorioallantoic membrane: the gelatin sponge/chorioallantoic membrane assay. *J Vasc Res* 34:455–463
51. Facchiano F, Benfenati F, Valtorta F, Luini A 1993 Covalent modification of synapsin I by a tetanus toxin-activated transglutaminase. *J Biol Chem* 268:4588–4591